094048
(10)

6/8/2006

APPLICATION OF TIME-DOMAIN AIRBORNE ELECTROMAGNETIC INDUCTION TO HYDROGEOLOGIC INVESTIGATIONS ON THE PAJARITO PLATEAU, LOS ALAMOS, NEW MEXICO, USA

Authors: W. Scott Baldridge[1], Gregory L. Cole[2], and Bruce A. Robinson[3], and George R. Jiracek[4]
[1]Earth and Environmental Sciences Division, D462, Los Alamos National Laboratory, Los Alamos, New Mexico 87545 USA. E-mail: sbaldridge@lanl.gov.
[2]Earth and Environmental Sciences Division, D462, Los Alamos National Laboratory, Los Alamos, New Mexico 87545 USA. E-mail: gcole@lanl.gov.
[3]Earth and Environmental Sciences Division, T003, Los Alamos National Laboratory, Los Alamos, New Mexico 87545 USA. E-mail: robinson@lanl.gov.
[4]Department of Geological Sciences, San Diego State University, San Diego, California 92182-1620 USA. E-mail: jiracek@moho.sdsu.edu.

Submitted: 8 June 2006

ABSTRACT

We conducted a time-domain airborne electromagnetic (**AEM**) survey to investigate the hydrogeology of a region of the semi-arid Pajarito Plateau of northern New Mexico. The geology of the area includes a thick (≤ 365 m) vadose zone in variably-welded volcanic tuff. Of particular interest were depths and lateral extent of perched aquifers in the vadose zone, and depths and pathways of infiltration to the regional aquifer. The AEM results provide an image of the electrical resistivity of the Plateau, which ranged over three orders of magnitude (<20 to >2000 Ω-m), to a depth of at least 300 m. Borehole and surface-derived data allow the correlation of resistivity images with the hydrogeology of the Plateau.

As expected, water exerts a major control on resistivity. However, the presence of large amounts (≤ 90%) of clay (dominantly smectite) in some units, in conjunction with water, also has a major effect on the AEM resistivity values, lowering resistivity (to ≤30 Ω-m) more than the presence of clay-free saturated zones alone. Because of the resulting low resistivity, we are able to better delineate a large, known volume of clay-altered volcaniclastic rock and postulate the presence of another. Resistivity values of 100-300 Ω-m correlate with depths to saturated zones where no clay is present, but, because of the limited sensitivity of the AEM technique, do not allow us to distinguish between one large or several smaller perched groundwater zones and the underlying regional zone of saturation. We imaged a region of major infiltration related to a sewage-treatment plant and to near-surface hydrogeologic conditions conducive to infiltration, and correlated with a region of preferential transport of anthropogenic chemicals through the vadose zone.

14497

AEM data provide an important synoptic view of the shallow (few hundred meters) resistivity structure of the Plateau. Although interpretation of the data is not unique, when combined with borehole geologic, hydrologic, and geochemical data it can provide relative depths to saturated zones, delineate regions of high clay content (zones of alteration), and image regions of recharge to the regional aquifer.

INTRODUCTION

Investigation of groundwater resources beneath the Pajarito Plateau of northern New Mexico is increasingly important because of (1) contamination from historical operations of the Los Alamos National Laboratory (**LANL**), located prominently on the Plateau, (2) recognition that the Plateau is an area of significant recharge to the regional groundwater reservoir, and 3) rapidly increasing population in the area with attendant demands on groundwater supply. Long-term efforts are underway to assess the quantity and quality of groundwater beneath the Plateau, and in particular to characterize surface and subsurface sources of contamination and potential pathways by which contamination can reach the regional groundwater aquifer (LANL, 1998). This characterization will be used to develop appropriate mitigation strategies where necessary.

Of particular importance to the present work is the characterization of alluvial and perched aquifers in the vadose zone overlying the regional groundwater aquifer. Alluvial and perched aquifers refer respectively to unconfined groundwater in the alluvium of stream channels, and in underlying sediments or bedrock and separated from an underlying main body of groundwater by an unsaturated zone (the vadose zone). This thick (200-365 m) zone, once thought effectively to isolate alluvial water from the regional aquifer (Purtymun, 1995), provides a significant delay in the time required for alluvial water to percolate through the vadose zone. However, contamination by both radiogenic and nonradiogenic species resulting from historical activities at LANL and from municipal sewage-treatment plants has been observed in perched groundwater and in the regional aquifer beneath the Plateau (LANL, 1998). Most of the discharged contaminants are thought still to reside in the vadose zone. Major limitations on understanding transfer of contaminants to the regional aquifer are the lack of knowledge of vertical and lateral extent of perched aquifers, the connections between them, and the overall hydrologic properties of the subsurface geologic units.

To date, characterization of the subsurface hydrology of the Plateau has proceeded mainly through an ambitious campaign of shallow (tens of meters or less) to deep (>500 m) exploratory boreholes and monitoring wells (LANL, 1998; Robinson et al., 2005a). Drilling has yielded a wealth of valuable geologic, geochemical, geophysical, and hydrologic data. Disadvantages of a drilling program include the high cost of drilling, and the risk of ineffectively locating boreholes due to inability to predict the location, lateral extent, and depth of perched water. In addition, the large area (111 km^2) over which historical operations at LANL were conducted precludes adequate characterization of the subsurface exclusively by drilling.

The present report describes the relatively new application of time-domain airborne electromagnetic (**AEM**) technology to the characterization of groundwater. AEM was undertaken because of the dependence of electrical resistivity on water-saturated porosity and the ability of airborne-techniques to survey large areas in short

RECEIVED
OCT 24 2006
By

periods of time, making it possible to determine efficiently the lateral extent of known perched aquifers and to search effectively for additional zones and pathways. The technique also allows for extrapolation of hydrogeologic properties between boreholes or other areas of ground control. AEM has been used successfully in several other areas to characterize groundwater resources (Bultman et al., 1999; Paine, 2000, 2003; Deszcz-Pan et al., 2001; Smith et al., 2004), suggesting that its application on the Plateau was likely to yield useful results. Specific questions include: does evidence exist for canyon-floor recharge in particular areas of interest, can zones of perched water be resolved and distinguished from the regional groundwater aquifer, and what is (are) the overall control(s) on electrical resistivity on the Plateau? Our expectation was that the resulting evaluation of the AEM survey would assist the management of a groundwater characterization program, thereby reducing overall costs. The present detailed comparison of the AEM results with ground- and borehole geophysical and hydrogeologic data constitutes a valuable case study on the application of the AEM technique.

GEOLOGIC AND HYDROGEOLOGIC SETTING

Geologic setting and stratigraphic units

The Pajarito Plateau is located east and southeast of the Jemez Mountains near the western margin of the Española basin (Fig. 1), one of the structural basins of the late Cenozoic Rio Grande rift (Baldridge et al., 1995). The Plateau comprises a gently east-dipping surface sloping from an elevation of 2380 m adjacent to the Jemez Mountains to 1890 m on the east (Fig. 1). The eastern margin stands 90-275 m above the Rio Grande. Because the Plateau is underlain dominantly by poorly lithified volcanic tuff and volcaniclastic sedimentary rocks, it has been deeply incised by intermittent and perennial tributary drainages of the Rio Grande, leaving finger-like mesas between.

The principal bedrock units of the Plateau consist of, in ascending order (Fig. 2): (1) Santa Fe Group, (2) an older fanglomerate unit, (3) pumice-rich volcaniclastic sediments, (4) Puyé Formation, including the Totavi Lentil, (5) Otowi (lower) Member of the Bandelier Tuff, (6) epiclastic sediments and tephra of the Cerro Toledo interval, (7) Tshirege (upper) Member of the Bandelier Tuff, and (8) mesa-top and stream-bottom alluvium, colluvium, and soil. Volcanic rocks, breccia, and tuff of the Cerros del Rio volcanic field and of the Tschicoma Formation are intercalated within the stratigraphic section in the eastern and western parts of the area, respectively.

The Miocene Santa Fe Group comprises dominantly continental arkosic conglomerate, sand, silt, and clay, with interbedded volcanic ash beds and minor lava flows (Cavazza, 1989; Ingersoll et al., 1990). It ranges in age from approximately 19 to 5 m.y. Several boreholes on the eastern Pajarito Plateau encountered sequences up to 41 m thick of basaltic flows interbedded with sedimentary rocks of the Santa Fe Group.

The older fanglomerate and pumice-rich volcaniclastic sediments are new units with provisional, informal names (Broxton and Vaniman, 2005). These units are generally similar to the overlying Puyé Formation, but are older than rocks normally assigned to it.

The Pliocene Puyé Formation consists mainly of fanglomerate deposits of poorly sorted boulders, cobbles, and coarse sand of dacitic to latitic debris eroded from the contemporaneous Tshicoma Formation to the west (Turbeville et al., 1989). It contains numerous interbedded lapilli tuff beds, and lahar and lacustrine deposits. The lower part of the Puyé Formation includes fluvial cobbles and boulders of Precambrian quartzite and crystalline rocks (Totavi Lentil).

The Quaternary Bandelier Tuff, which is the uppermost bedrock unit over wide areas of the Pajarito Plateau, consists of two separate fallout and ash-flow tuff units separated by epiclastic sediments and tephra of the Cerro Toledo interval. The lowermost unit of the Bandelier is the Otowi (or lower) Member (1.613 ± 0.011 Ma; Izett and Obradovich, 1994), the base of which consists of up to 15 m of pumice and ash fallout deposits. It is overlain by nonwelded ash-flow tuff units and lacks the cooling joints which characterize much of the Tshirege member (below). The Otowi Member ranges up to 128 m thick (Birdsell et al., 2005).

The upper, Tshirege, Member (1.223 ± 0.018 Ma, Izett and Obradovich, 1994) consists of a 0.3-1.2 m-thick basal fall-out tuff, which is overlain by ash-flow tuffs. The ash-flow tuffs comprise a sequence of nonwelded to densely welded subunits. Within welded units, the degree of welding generally increases from west to east across the Plateau. Welded units are commonly more fractured than the intervening nonwelded units; fractures present in welded units typically do not continue into overlying and underlying nonwelded units. Densely welded units are typified by porosities of 17-40%, unsaturated volumetric water contents of 3-12%, and low saturated hydraulic conductivity (10^{-6}-10^{-9} cm/s) (Birdsell et al., 2005). Nonwelded units lack the pervasive cooling joints that characterize welded portions of the Tshirege Member (Birdsell et al., 2005). Overall, the Bandelier tuff (and the included Cerro Toledo sequence) ranges in thickness from 0 to 275 m.

Intercalated between the two members of the Bandelier tuff is the Cerro Toledo sequence, typically ranging from 3 to 14 m thick. It consists of primary fallout- and pumice-fall deposits, tuffaceous sandstone and siltstone, and poorly-sorted sand, gravel, cobbles, and boulders derived from the Tshicoma Formation.

Subsurface hydrogeologic conceptual model

Regional aquifer.--A vadose zone ranging from about 365 m thick beneath the western edge of the Plateau to about 180 m beneath the eastern edge separates the surface of the Pajarito Plateau from the regional water table. In elevation, the water table declines from approximately 3000 m along the western margin to about 1650 m at the eastern extent (Purtymun, 1995). The surface of the regional aquifer, which lies dominantly within or between sediments of the Puyé Formation and Santa Fe Group, has been the chief source of drinking and industrial water for Los Alamos since the 1940s (Purtymun, 1984), and is increasingly well characterized because of an ambitious program of drilling on the Pajarito Plateau (Purtymun, 1995; LANL, 1998; Robinson et al., 2005a). This program has confirmed the existence of unconfined, water-table conditions at most locations in the study area.

The exact sources of recharge to the regional aquifer are not known with certainty. However, a significant proportion of the total recharge probably occurs along

the basin margin at higher elevations, including the mountain-front on the western edge of the study area, where precipitation rates are highest (Keating et al., 2005). In these areas, preferential recharge is likely along fractures and faults associated with the Pajarito fault zone. In addition, recharge on the Plateau, estimated from streamflow and other information (Kwicklis et al., 2005), could contribute up to 23% of the total recharge to the aquifer. At these lower elevations, which include the area covered by the AEM survey, recharge occurs preferentially along canyons.

Alluvial groundwater.—In some canyons, such as Cañon del Valle and Los Alamos, Pueblo, and Mortandad Canyons (Fig. 3), infiltration of surface water from streams and from spring and effluent discharges maintains shallow groundwater in canyon-bottom alluvium and underlying bedrock units (mainly Bandelier Tuff). With the exception of Mortandad Canyon, the headwaters of these canyons (termed "wet canyons") lie in the Jemez Mountains west of the Plateau, hence the canyons are typified by perennial streams in their upper reaches and/or by frequent runoff during precipitation events. In Mortandad and Pueblo Canyons, perennial water flow is supplied or augmented by effluent discharge. Depending on the underlying geological units, relatively high (0.1 to >1.5 m/yr) percolation rates from the saturated zones to the underlying unsaturated zone may occur (Birdsell et al., 2005). In contrast, in canyons which head on the Plateau and are thus occupied only by ephemeral streams (termed "dry canyons"), alluvium may be saturated only seasonally or remain unsaturated. Depletion by evapotranspiration and movement into the underlying bedrock units limit the horizontal and vertical extent of the alluvial groundwater. Infiltration rates are estimated at 1-10 mm/yr (Birdsell et al, 2005). From limited borehole data, we infer that alluvial aquifers, where present, do not extend laterally beyond the widths of the canyons.

Intermediate-depth groundwater—Local zones of saturation occur at depths ranging from 30 m to 272 m throughout the vadose zone beneath the western and central Pajarito Plateau, and perhaps beneath other parts of the Plateau as well. Intermediate-depth perched zones occur particularly beneath or adjacent to major canyons, including Los Alamos, Pueblo, Sandia, and Mortandad Canyons, and Cañon de Valle. Thickness of these zones are highly variable, ranging from ~1 m to >122 m (Robinson et al., 2005b). Whether they represents subsurface pathways in which water percolates laterally along perching horizons en route to greater depths, or whether the saturated zones are isolated pockets of relatively stagnant water residing within the vadose zone is uncertain (Robinson et al., 2005b). Intermediate-depth groundwater bodies are typically found in the Puyé Formation, in the Cerros del Río basalts, and at the base of the Bandelier Tuff (e.g., Broxton et al., 2001b; Longmire et al., 2001; Robinson et al., 2005b). Although data are sparse, fewer intermediate groundwater zones occur beneath mesas, where infiltration rates are much lower. In addition, water from many of the intermediate-depth zones bears the chemical signature of the overlying alluvial groundwater, including the presence of contaminants from LANL operations. Therefore, a requirement for intermediate-depth perched water to exist appears to be a combination of high local infiltration rates and the presence of low-permeability barriers to downward vertical flow. However, the vertical and lateral extents of individual saturated zones, and possible hydraulic connections among them, cannot be mapped with available borehole information.

Perched water in the vadose zone and the shallow regional aquifer share common hydrogeologic units in many locations. Both for perched vadose-zone water and for the regional aquifer, laterally discontinuous heterogeneities may significantly impede flow in the vertical direction, forcing water to migrate laterally except in high-permeability "windows." In the vadose zone, downward-percolating fluid may hit these low-permeability layers and be diverted laterally. In the regional aquifer, west-to-east gradients result in large-scale flow toward the Rio Grande, but local heterogeneities similar to those in the vadose zone may direct water in other directions on a more restricted spatial scale. Thus, pathways in the vadose zone and in the shallow regional aquifer probably comprise a system of complex, interconnected unconfined flowing zones with significant lateral migration rates and with local flow directions that may deviate significantly from the regional flow direction. Mapping the locations of these zones within the vadose zone is an important component in assessing the nature of subsurface contaminant pathways.

Infiltration mechanisms—Infiltration along canyons may occur by one or several of the following mechanisms: unsaturated flow, saturated flow through particularly permeable units, or flow through fractures and faults (Birdsell et al., 2005). Infiltration through the vadose zone in the Bandelier Tuff is generally controlled by flow through the matrix, despite the abundance of fractures in some units (Robinson et al., 2005b). Local infiltration may be enhanced by fracture flow at the surface, but water initially present in fractures quickly soaks into the rock matrix. By contrast, hydrologic behavior under ponded conditions in basaltic rocks is controlled by fractures rather than by the matrix, resulting in more rapid movement of water and presumably higher infiltration rates as long as a supply of surface and shallow alluvial water is available. Migration of contaminants from the surface to intermediate-depth perched zones has occurred on time scales of days to years where basalt is present in the shallow subsurface (LANL, 1998; Robinson et al., 2005c; Levitt et al., 2005; Stauffer and Stone, 2005).

The infiltration rate from mesa-top sites on Bandelier Tuff to perched aquifers and to the regional aquifer is probably much smaller than infiltration rates from canyons because of significant runoff and evapotranspiration processes (Birdsell et al., 2005). However, at mesa-top outfalls and settling ponds where significant anthropogenic discharges over decades have occurred, percolation to intermediate-depth and possibly to the regional aquifer has occurred (LANL, 2003). At these sites, pathways may include fractures and matrix flow directly to depth, or lateral transport to canyons and subsequent percolation from the alluvial groundwater zone to depth. From surface sources, water may migrate downward either along fractures or as matrix flow through the tuff until it reaches surge beds (deposits resulting from turbulent, gas-rich transport), pumice beds, or sediments of the Cerro Toledo interval. Water may then move laterally within these units until it reaches other vertical pathways, whereupon it continues to migrate downward. "Fast" pathways may be provided by open fractures in the Bandelier Tuff. Contaminants from mesa-top (or possibly canyon-bottom) sites near the western Pajarito Plateau have reached a perched aquifer at a depth of approximately 213 m in <50 y (Anonymous, 2003a). Overall, however, we expect that the near-surface driving force for water percolation to great depths to be much greater from canyon bottoms than from mesa tops. Therefore, water sources identifiable with large-scale geophysical techniques such as the AEM survey described herein are more likely to originate from canyon bottoms.

METHODS AND APPROACH

Time-Domain Airborne Electromagnetic Survey

A time-domain airborne electromagnetic (AEM) survey was flown September 4-11, 2001, by Fugro Airborne Surveys Corporation using a MEGATEM II® time-domain airborne EM system mounted on a deHavailland Dash 7 turbo-propeller aircraft. A total of 762 line-kilometers of data were collected during 13.5 hours of flight time (Fig. 3). Flight and survey parameters are provided in Table A1 and acquisition parameters in Table A2 (Appendices). The survey parameters were expected to yield conductivity information to a depth of ≥ 300 m below the surface given the expected conductivity values.

An inversion (or imaging) technique was used to best fit the data to a geoelectric model. A one-dimensional (1-D) geometry was used for all models to represent the gently east-southeast dipping, layered stratigraphy of the resistive Bandelier Tuff (with possible enclosed zones of relatively conductive vadose water). Models did not take into account the constraints of the hydrologic and hydrogeologic site data. A 1-D model is less appropriate for the deeper, pre-Bandelier units, which tend to be laterally less continuous.

Sensitivity models (Fig. 4) using conservative values for resistivity show the expected signal response for the z-component of the B-field for 50 Ω-m, 3-D layers 20 m thick with (a) lateral dimensions of 2.5 km at depths between 200 and 300 m, and (b) lateral dimensions of 200 m at depths of between 50 and 150 m. These cases may be proxies, respectively, for the regional groundwater aquifer and for perched saturated zones. The model results indicate that we can expect to image km-scale saturated bodies or clay zones in the vadose zone, but that 100 m-scale bodies would probably elude detection.

Data Processing

Three approaches were used in processing the airborne TEM data, the first by Fugro as a standard product provided as part of the data collection, and the others by Condor Consulting, Inc, of Lakewood, Colorado. In the Fugro processing, data from 20 channels of x- and z-coils were used to compute values of apparent conductance (conductivity x thickness) by fitting to a continuous thin-sheet model. These data were then fitted to a layered earth model to derive conductivity variations as a function of depth. Fugro's processing uses a proprietary, 1-D imaging technique described as a conductivity-depth transform method (**CDT**), which is based on the variation of the EM diffusion velocity with conductivity (Wolfgram and Karlik, 1995; Christiansen and Christensen, 2003). Conductivity data are presented as conductivity-depth transform (or CDT) sections for individual flight lines. Data from the CDT sections were combined to produce conductivity-depth slices at depths of 50, 100, 150, 200, and 300 m. The CDT technique assumes no initial model, and is fast and robust. This processing methodology can generally be improved upon with appropriate geologic control.

Processing by Condor used two independent processing applications, EM Flow and AirStem. EM Flow is a software application that fits a discrete- layered earth model to EM decay information on a fiducial-by-fiducial basis. The results are then displayed as conductivity-depth images (**CDI**), analogous to the CDT sections in the Fugro processing. For the present work only the z- (vertical-) secondary magnetic component was used. The x-component (horizontal component parallel to the flight line) was commonly corrupted by cultural artifacts in the study area. AirStem, a proprietary code of BHP Billiton, uses a formal 1-D inversion of airborne TEM. Results are also displayed as CDIs. Layer interfaces are chosen a priori and are held fixed. The code will invert z- or x-channel data, but to avoid cultural interference only z-channel data were used in this study. For this work the inversion model used 28 layers, with thickness increasing in roughly logarithmic fashion from the surface to depth. The shallowest and deepest layers were respectively 5 and 232 m thick. For comparison, in the depth interval 200-300 m the layers are 27-40 m thick, and at 400 m approximately 60 m thick. No geological or geophysical data were used to constrain the model.

This Work

We gridded the Fugro CDT and Condor EM Flow and AirStem CDI conductivity-depth data to construct 3-D data cubes using a locally developed FORTRAN program. Then, with an application we developed using public-domain OpenDX (www.opendx.org), we visually compared the AEM results with geophysical, geochemical, and hydrogeologic data. We compared data from more than 40 boreholes ranging in depth from 235 to >900 m. However, we selected wells in two subareas (Fig. 3) for detailed comparison of the AEM results with geological and hydrological data: (1) an area comprising portions of Bayo, Pueblo, Los Alamos, Sandia and Mortandad Canyons near the eastern edge of the survey area, and (2) a region near the junction of Cañon de Valle and Water Canyon. These areas were selected because each has a different combination of lithologic and hydrologic characteristics. Together they encompass a range of factors affecting the AEM data. Data used for comparison include borehole lithologic and induction logs, depths and thicknesses of saturated zones, laboratory determinations of gravimetric moisture content, clay content, and clay composition. In the following evaluation we focused on the AirStem data. Although the EM Flow results are different in detail from the AirStem results, they are not substantially different overall.

ELECTRICAL RESISTIVITY DATA

Electrical Resistivity of Rocks and Soil

Although the resistivity of naturally occurring earth materials varies by at least 12 orders of magnitude, near-surface values are typically in the range of 1 to1000 Ω-m. Thus, the variations measured on the Pajarito Plateau (Tables A3 and A4, Appendices), ranging from 7 Ω-m in the perched water of the Ceros del Rio basalt to ~ 2000 Ω-m in the nearly dry Bandelier tuff, are typical. Water, both through its intrinsic resistivity and through the degree of saturation of the host rock or soil, is the most important variable in

hydrologic resistivity studies because the solid rock matrix or soil grains are comparatively very good insulators. Consequently, the ions dissolved in water are the electric charge carriers responsible for the ability of the bulk material to conduct electricity. This mechanism is true for both clay-free and clay-rich formations. Other factors affecting the resistivity of surficial earth materials (e.g., McNeill, 1990) are porosity; texture, which influences pore space interconnectivity; temperature; and clay content.

The abnormally low resistivity of clay minerals is caused by mobile cations in the fluid that are required to balance the negative surface charge on most clay particles. Negative surface charge is caused by unsatisfied bonds on grain edges and crystal lattice substitutions on cleavage surfaces. The ion exchange capacity of a mineral is a measure of the number of cations required to neutralize this negative surface charge. Every mineral has an ion exchange capacity; clay minerals, especially montmorillonite and vermiculite, have large values. But, because the cation exchange phenomenon is surface-dependent, it is also greater for fine grain compared to coarse grain formations with identical volumes of the same clay mineral. Because both the mineralogy and grain size are important, both clay minerals and clay-size particles exhibit enhanced ion exchange capacity. In the presence of a fluid the adsorbed cations form a double layer attached to clay surfaces (Ward, 1990). One layer is immobile and fixed to the clay particles. The other layer, referred to as the diffuse layer, varies in concentration in the fluid as a decreasing function of distance from the clay surfaces. The diffuse cations are free to move under the influence of a voltage-causing electric field. These loosely bound cations effectively increase the charge density available for ionic conduction in the electrolyte. Such an additional contribution to the conductivity is referred to as surface conductivity or the double layer effect. It can exceed the conductivity of the normal water by many times and is thus of utmost importance in clay-rich zones. The effect is generally more important when the water conductivity, therefore the intrinsic ion content, or the porosity is low. When water is extracted from a formation, the measured conductivity of the sample is that of the intrinsic water conductivity, σ_w. It does not include any contribution from the exchange cations, which remain attached to the mineral grains. Therefore, measured water conductivity values such as reported in Table A3 should be considered as underestimates of the effective ionic conductivity when clay is present.

Surface- and groundwater

The electrical resistivity of stream water on the Pajarito Plateau tends to be relatively high (up to 100 Ω-m) because of its low content of dissolved species. Resistivity for stream discharge events in Cañon de Valle, measured over a four year period, ranges from approximately 11 to 100 Ω-m. Resistivity is constant or decreases slightly with distance downstream (LANL, 2003), but this variation is not important to the interpretation of the AEM data. Resistivity of extracted groundwater ranges from 7 to 132 Ω-m, and is not strongly dependent on the formation hosting the water.

Bedrock formations

Resistivity values of bedrock formations have been determined by a variety of surface soundings and surveys using galvanic, frequency-, and time-domain induction

techniques; and by borehole induction methods. Measured resistivity values in the vadose zone range from as low as 30 to nearly 2000 Ω-m (Table A4). The lowest values correspond to the Cerro Toledo sedimentary interval and gravimetric water contents of 10-47.4 wt.%. Although nominally in the vadose zone (i.e., not producing water in the borehole), the very high water content may indicate that local thin zones of saturated sediment were present.

In the Bandelier Tuff, resistivity ranges from ~300 Ω-m to nearly 2000 Ω-m for gravimetric water contents 2-4 wt.%, and from <10 to >1000 Ω-m for moisture values of ~10% (Gilkeson et al., 1996; Vaniman et al., 2005). The range in values probably reflects moisture content, clay content (Vaniman et al., 2005), and resolution of the technique (Gilkeson et al., 1996). Resistivity values are generally greatest below mesa tops, where unsaturated conditions exist. Values of ~1000 Ω-m or greater are likely to represent rock that is essentially "dry." Few data are available for the Puyé Formation or the Cerros del Rio basalts. Limited borehole induction data indicate that resistivity ranges from 19 to 53 Ω-m for the Puyé Formation. These values may suggest a fairly high moisture content, water salinity, and/or clay content. For the Cerros del Rio basalts, resistivity ranges widely, depending on water content and clay content.

Thus, overall the range of resistivity values for water and rock units of the Pajarito Plateau exceeds three orders of magnitude. Where gravimetric water data are available, resistivity of rock units broadly correlates inversely with water content (Table A4). As expected, surface and groundwater generally have lower resistivity compared to bedrock units (Table A3), but locally the presence of clay (in combination with water) exerts significant control on resistivity (see discussion above). High clay content can cause low values of electrical resistivity (Vaniman et al., 2005). However, over the Plateau as a whole (with prominent exception, to be discussed below), we infer that water content is the dominant control on the resistivity measured in the AEM survey. Because of the range of resistivity values observed and because water is an important control on low resistivity values, we conclude that EM methods are suitable and effective for surveying for the presence of groundwater in the vadose zone over broad areas of the Pajarito Plateau. However, the competing effects of dissolved species, porosity, permeability, clay content and other variables such as anisotropy and equivalence relations in EM measurements make quantitative estimates of water content ambiguous unless other data such as borehole results provide control.

RESULTS AND DISCUSSION

Considerable variation in resistivity over the survey area occurs at any given depth. For example, resistivity values in AirStem inversion results at a depth of 200 m range from <10 to >1000 Ω-m (Fig. 5). In this section we compare the AEM AirStem results to relevant hydrologic, geologic, and geophysical data. In making these comparisons we have considered electromagnetic noise from the Laboratory and town-site infrastructure. Noise is especially evident in the Los Alamos and White Rock residential/business areas, and in the transportation and communications corridor between them (Fig. 5). We selected the two subareas described above for detailed comparisons and interpretation, mainly comparing the AEM results with data derived from boreholes.

For these subareas, noise was not a significant problem because most of the wells lie outside of the high-noise corridors. Interpretations derived from these subareas can then be applied to other surveyed regions of similar geology which are not discussed in detail in this paper.

Subarea 1 ("low resistivity")

The first subarea, encompassing an area from Bayo to Mortandad Canyons near the eastern edge of the survey area, was selected because it exhibits a very strong AEM *low-resistivity* signature at relatively shallow depths. Several flight lines cross this area, but we illustrate line 112 (Figs. 3, 5, 6), which extends approximately through boreholes Otowi-1 (Bayo Canyon), R-9 (Los Alamos Canyon), and R-12/PM-1 (Sandia Canyon) (Fig. 3). Along this line, the low-resistivity (<30 Ω-m) area extends from Bayo Canyon, where it is continuous upward to the surface, 13 km southward to Mortandad Canyon. To the east the low-resistivity zone extends to the edge of the survey area (Fig. 5). Westward, it includes R-5 in Los Alamos Canyon, and is bounded between R-12 and R-13 in Sandia Canyon. Borehole R-12 is a special case in that a low-resistivity zone (< 300 Ω-m) is present in the uppermost ~100 m below the surface in the AEM data. The effect could be to mask other low-resistivity regions of the vadose zone below, if present. Also, because conductive zones attenuate the EM signals more than resistive zones, the AEM system does not sound as deeply where a shallow high-conductivity region is present. In this subarea, the 30 Ω-m contour (approximately marking the top of a thick conductive zone) typically occurs between 168-244 m below ground surface, including in borehole R-12 (Fig. 8). Generally, resistivity increases in depth toward the west (Figs. 9, 10).

Compared to other parts of the survey area, this subarea is relatively "wet." Los Alamos Canyon, which begins in the Jemez Mountains west of the Plateau, contains a perennial stream in its upper reach and has a substantial alluvial aquifer over much of its length. Relatively low resistivity along the length of Los Alamos Canyon is observed at depths of 200 m and 300 m (Fig. 5), consistent with the conceptual model of increased infiltration along wet canyons (Birdsell et al., 2005) and with site-specific studies of Los Alamos Canyon (Robinson et al., 2005c). The headwaters of Mortandad Canyon are located on the Pajarito Plateau; thus, this canyon has natural flow only during runoff events. However, it is fed by an active outfall and has perennial flow in its upper reach to the west of subarea 1.

All boreholes in this subarea encountered at least one and typically multiple perched zones above the zone of regional saturation (Fig. 8). Boreholes were sited either on canyon-floor alluvium or on Bandelier Tuff, and all encountered a thick section of Cerros del Rio basalts (Fig. 8). In this area the Cerros basalts are underlain by fanglomerate of the Puyé Formation or, as in R-8, are both overlain and underlain by the Puyé. The Puyé Formation is, in turn, underlain by the informally named pumice-rich volcaniclastic sedimentary unit described earlier, and by basalt and relatively fine-grained sediments of the Santa Fe Group. In all boreholes, perched zones ranging in thickness from 0.3 m to 29 m occur above the regional saturated zone within one or more of the following units: Bandelier Tuff, Cerros del Rio basalt, Puyé Formation, and pumice-rich

volcaniclastic unit. Depth to the regional zone of saturation ranges between 184 and 245 m, coinciding within ~10 m with the 30 Ω-m contour (Fig. 8).

Compared to other parts of the survey area, the pumice-rich volcaniclastic unit in this area underwent significant alteration to clay minerals (Fig. 9.) Clays consist dominantly or exclusively of smectite, with kaolinite/halloysite also present (Vaniman et al., 2005). In some depth intervals (e.g., ~183 m depth in R-9/9i, and 122-200 m depth in R-5), the clay content of the pumice-rich unit approaches and locally exceeds 90% (Fig. 8). Clay alteration is likely to lead to low permeability and perching. Also, the fact that Bandelier Tuff is not present at all locations (e.g., R-9/9i) allows percolation directly into fractured basalt and the highly heterogeneous Puyé Formation at these locations, thereby yielding larger infiltration than locations upstream where the Tuff underlies the canyon. Thus, the location of this wet region, in which numerous perched zones are present (Robinson et al., 2005b), is consistent with both the presence of clay alteration and of an enhanced zone of infiltration.

Westward from subarea 1 the resistivity as determined by AEM increases sharply at all depths (Fig. 5). Despite the fact that borehole R-13 in Sandia Canyon is located only about 2 km west of R-12, resistivity recorded adjacent to R-13 by both the AEM survey and by downhole induction logging is much higher (Fig. 10). In general, the stratigraphy of R-13 is similar to that of R-12. However, two significant differences occur. First, no perched zones were encountered in the vadose zone above the regional saturated zone. Thus, R-13 is generally "drier" than R-12. Second, despite the fact that a 21 m-thickness of the pumice-rich unit is present at R-13, it is almost entirely unaltered. Virtually no clay is present in this unit at this location.

Subarea 2 (generally "resistive")

In contrast with subarea 1, subarea 2, comprising a region near the confluence of Cañon de Valle with Water Canyon (Fig. 5), was selected as an example of an area which generally has a *resistive* signature at intermediate depths. The resistivity measured by AEM at regional water table depths (~350-380 m) ranges from ~ 70 to 330 Ω-m (Fig. 11). Three boreholes were selected to characterize this area: CdV-R-37-2, CdV-R-15-3, and R-19 (Fig. 11). All are located at mesa-top sites. In all boreholes a thick section of Bandelier Tuff overlies sedimentary rocks of the Puyé Formation. Volcanic and volcaniclastic rocks of the Cerros del Rio and/or Tschicoma Formations are intercalated within or underlie the Puyé. In contrast with subarea 1, no significant amounts of clay are present in any of these formations.

Compared to boreholes in subarea 1, these holes are generally drier, and little or no perched water is present in the vadose zone. CdV-R-37-2 encountered no zones of saturation above the regional water table at 365 m. CdV-R-15-3 encountered several possibly saturated zones in the vadose region when drilled, but none is actively producing water now. Resistivity values are low between depths of 180 and 366 m, which may indicate that the initially saturated zones remain wet but are presently unsaturated. Resistivity determined by AEM is ~90 Ω-m near the water table at 379 m-depth, compared to 150-200 Ω-m determined by borehole induction.

R-19 also encountered zones of perched water above the regional water table. Borehole induction resistivity values are relatively low (150-300 Ω-m) within this region

(i.e., below ~244 m) except for some high-resistivity excursions in intervals within the Puyé Formation and the Tertiary basalt. At the present time only the lower of the two perched zones produces water. Resistivity is low within the regional saturated zone (Figs. 11). Resistivity determined by borehole induction compares well with the AEM resistivity (~260 Ω-m) determined at the water table.

Other observations

With a generally favorable correlation established between the AEM data and known locations of perched water and clay-altered rock, we now make two additional correlations in locations where the data coverage is sparser. First, the southern and central parts of the survey area are characterized by very resistive AEM signatures (Fig. 5). Most of the canyons in this region head on the Plateau and thus are relatively dry, suggesting that they are regions of low infiltration. The inferred low infiltration is consistent with the absence of perched water in the few boreholes in this area and with the resistive AEM signature. Second, the two northwest-southeast flight lines extending west of the main study area suggest zones of lower resistivity directly east of the mountain front (Fig. 5). We expect regions of increased recharge in this area due to enhanced precipitation and to fault and fracture pathways related to mountain-front faults (Kwicklis et al., 2005). The lack of complete survey coverage in this region precludes a more definitive assessment of the effects of increased recharge and infiltration at the mountain front.

SUMMARY AND CONCLUSIONS

In this study we assume that lithologic parameters such as porosity, permeability, and grain size within individual rock units at the scale of the AEM survey are similar in all parts of the survey area, except where noted. In the clay-rich area (subarea 1), this condition is almost certainly not met because the grain size of pumice-rich volcaniclastic unit is much finer where altered (Vaniman et al., 2005). We also assume that the conductivity (and salinity) of the water is similar in all parts of the survey area. From data in Tables A3 and A4, we infer that no major differences in resistivity occur in the formation water. Future work will be required to evaluate the extent to which these assumptions are met, and their consequences.

AEM with the MEGATEM system is generally useful for indicating the presence of groundwater. Low values of resistivity (< 300 Ω-m) broadly correlate with the presence of saturation, either as perched aquifers in the vadose zone or as the regional saturated zone. This relationship is especially apparent in drier areas, where little or no perched water is present in the vadose zone (R-13, Fig. 10; also subarea 2, Figs. 11). In "wetter" areas where thick or multiple perched zones are present (Fig. 8), low resistivity values (≤ 300 Ω-m) occur at or near the top of the region of perched aquifers (e.g., R-9/9i, Fig. 8) or may extend all the way to the surface (R-5, R-8). In these boreholes the low-resistivity signal may be enhanced by the presence of clay. Although a low-resistivity (<300 Ω-m) zone occurs in the upper 100 m of borehole R-12, we rule out the presence of saturation as the cause, because no shallow perched zone is recognized in this

borehole (Broxton et al., 2001b). Low clay contents typify the upper 40 m (Broxton et al., 2001b), but the remainder of this interval has not been analyzed. Therefore, a high clay content with enough water to wet the grains could potentially explain the low resistivity in this interval. Alternatively, this low resistivity signature could result from EM noise. At present we are not able to distinguish between these possibilities. Nevertheless, the AEM resistivity at the water table in R-12 is ~30 Ω-m, in good agreement with nearby boreholes R-9/9i, R-5, and R-8.

Because resistivity is resolved over broad depth intervals, within which one or several saturated zones of variable thickness may occur, the correlation of ~300 Ω-m with saturation is empirical only. It cannot be expected to correspond to the resistivity of specific hydrogeologic units. For example, a resistivity of 280-300 Ω-m occurs in the Puyé Formation in boreholes R-13 (Fig. 10) and R-19 (subarea 2, Figs. 11), but in R-9/9i the 300 Ω-m occurs in Cerros del Rio basalt. Similarly, in subarea 1 (Fig. 8), the 30 Ω-m contour occurs in the pumice-rich volcaniclastic unit (R-12 and R-9/9i), basalt interbedded in the upper Santa Fe Group (R-5), and the Puyé Formation, all within a distance of < 0.5 km. Also, because of the depth resolution, the AEM survey cannot be expected to spatially resolve closely spaced or thin perched zones from each other or from the regional zone of saturation. For example, we attribute the fact that no unique correlation exists between a resistivity value and perched zones in subarea 1 (Fig. 8) to, in part, the relatively coarse resolution of the AEM technique. In effect, the low-resistivity signal is smeared out over a depth interval across perched and regional water tables.

In this work we find that very low values of resistivity occur in regions of high clay content. In these areas, resistivity of 30 Ω-m is typical at depths approximately corresponding with the top of the zone of regional saturation. Low resistivity values determined by AEM correlate reasonably well with borehole induction data (Fig. 8). We infer that that these low values occur because of the *combined* effect of both water and clay. Such low values are compatible with the measured resistivity of water extracted from formations (<10 Ω-m in some units; Table A3), and also with the low values expected from clay minerals (~1-10 Ω-m).

Correlation of the low-resistivity signal in the AEM data to clay-rich (altered) zones in the Puyé Formation is very important, because it allows us to extrapolate the boundaries of the clay-rich region beyond where it has been recognized by drilling. Our preliminary conclusion is that this clay-rich zone extends from Bayo Canyon (and may extend further north) southward 13 km to Mortandad Canyon. To the east it extends to the edge of the survey area and was not bounded by the AEM survey. Westward, it includes R-5 in Los Alamos Canyon, and is bounded between R-12 and R-13 (Figs. 5, 10), for a total east-west dimension of at least 2.4 km. The clay-rich zone or zones occur primarily in the pumice-rich volcaniclastic unit beneath the Puyé Formation. This zone is expected to have hydrologic significance, with such a zone almost certainly having a lower permeability than the corresponding unaltered rock. In the vadose zone, low permeability will be correlated with increased propensity for perching and lateral diversion of water; in the regional aquifer, this effect would result in higher gradients in the direction of flow. The vadose zone observations are consistent with this concept, whereas the regional aquifer gradients are complicated by the effect of supply-well pumping, which changes the gradients from their pre-development conditions.

Another smaller but distinct region of very low resistivity region occurs in the southeastern corner of the survey area southwest of White Rock, and is well imaged at a depth of about 300 m (Fig. 5, 6). It extends approximately 2.7 km in a north-northeast direction and is about 1.8 km in width. The zone appears to be bounded on all sides, at least at the 200 m depth, by the AEM survey. Although not intercepted by boreholes, based on the analysis of the conductive zone in subarea 1 we tentatively interpret this low-conductivity region also as resulting from high clay content in combination with water. Because the clay-rich parts of the pumice-rich volcaniclastic unit (or other formations) have reduced porosity and permeability (Vaniman et al., 2005), they may have an important effect in controlling aquifer characteristics and flow paths in perched aquifers and in the regional aquifer on the Pajarito Plateau. Thus, integration of these regions of reduced permeability into regional groundwater flow models will be important.

Pueblo and Bayo Canyons are areas of very low resistivity (<30 Ω-m) (Fig. 5). In Pueblo Canyon, a low-resistivity area is situated approximately 1.5 km downstream of a municipal sewage treatment plant and extends northeastward beneath Bayo Canyon. The low-resistivity zone is contiguous with the resistivity-low of subarea 1. Because of the proximity of this zone with a wetland (and alluvial aquifer) downstream from the sewage treatment plant, we speculate that the low-resistivity area is an area of significant infiltration from the plant and recharge to the vadose zone. At greater depth (300 m, Fig. 5) the low-resistivity zone is centered 2 km farther south, between Los Alamos and Sandia Canyons. Low resistivity in this region may also result from enhanced infiltration in lower Los Alamos and Pueblo Canyons, where the canyon bottom is cut directly into Cerros del Rio basalts (Robinson et al., 2005c). The importance of this result is magnified by the presence of contamination (tritium, percholorate, and nitrate) that has reached the regional aquifer in this region. The rapid (<60 yr) transport to the aquifer of mobile contaminants through the vadose zone is consistent with the results of the AEM survey, and suggests that this geophysical technique may provide constraints on the nature and extent of contamination.

Finally, the resolution of the AEM technique is not sufficient to resolve questions about infiltration mechanisms, i.e., fracture- vs. matrix flow. Although we postulate that major infiltration may occur over a broad zone 1-2 km downstream from the waste-water treatment plant and in other zones in Los Alamos and Pueblo Canyons, recharge could occur through numerous fractures distributed over this volume or by flow through the matrix, or both. Fracture studies of exposed units of the Bandelier Tuff show that fracture densities can range from 20 to more than 600 fractures per 30 m and fracture apertures from 0.1-100 cm (Wohletz, 1995; Lewis et al., 2002; Walters, 1996). The scale of the survey (along-line sampling interval of 17.5 m) and size of the EM transmitter loop (406 m^2) do not allow individual fractures or fracture zones to be imaged. Where infiltration occurs directly onto basalts, the mechanism is almost certainly fracture flow, although this conclusion is based on direct observations and basic hydrologic principles, rather than as a result of the AEM survey.

In summary, the AEM data provide a robust picture of the electrical conductivity of the upper few hundred meters below the surface of the Pajarito Plateau. Although the survey design does not have the resolution to image thin, closely spaced perched saturated intervals in the vadose zone (at least not for the thicknesses and numbers of zones present on the Pajarito Plateau), the data do provide a guide to depth to saturation.

Generally the resistivity values measured by the AEM survey are compatible with the much higher-resolution downhole induction resistivity logs. If the interpretation that very low resistivity (~30 Ω-m) is correlated with high clay content is correct, then the AEM data also provide a very useful tool for discerning zones of high clay content in the pumice-rich volcaniclastic unit, with good spatial resolution. Future work should include a more detailed analysis of lithologic controls, such as porosity, permeability, and grain size, on resistivity in places like Los Alamos and Mortandad Canyons, where a wealth of ground-based data is available.

ACKNOWLEDGMENTS

We thank D. J. Hollis for her role in initiating the AEM survey. J. G. Paine (Texas Bureau of Economic Geology) was a continuing source of guidance, technical information, and encouragement for this work. P. R. Romero, R. Steens, and E. F. Darling provided invaluable help with permitting, logistical, and safety issues for this complex survey. We appreciate the dedication of D. Beattie, D. Fountain, J. Rowe and the flight/field crew (D. Wiens, S. Christeas, R. Williams, A. Proulx, B. Fisher, and N. Craig) of Fugro Airborne Surveys for a professional, efficient, and safe airborne survey, and to R. Irvine and K. Witherly of Condor Consulting, Inc., for expert processing of the data. We also thank R. S. Smith (Fugro) for forward-modeling interpretations of the AEM data to assist with determining the sensitivity of the technique, and for comments on an early version of the manuscript. We are greatly indebted to D. T. Vaniman and D. E. Broxton for providing access to and assistance with the accumulated hydrogeologic data and for their invaluable help with interpretation of the airborne data. D. Vaniman provided unpublished data as well as important comments on early versions of this manuscript. Funding for this work was provided by the U.S. Department of Energy for the LANL Environmental Restoration Project and LANL Groundwater Protection Program.

APPENDICES

Table A1. Survey and flight parameters for airborne TEM and magnetic surveys.

Principal line spacing	100 and 200 m
Principal line direction	020° azimuth
Tie-line spacing	~2000 m
Tie-line direction	305°
Survey speed	70 m/s (125 knots)
Aircraft and transmitter height (nominal)	120 m
Magnetic sensor height (nominal)	75 m
EM sensor height (nominal)	70 m
Receiver trailing distance (behind center of transmitter loop) (magnetic)	80 m
Receiver trailing distance (behind center of transmitter loop) (EM)	125 m

Table A2. Acquisition parameters for MEGATEM system.

Transmitter-loop area (vertical axis)	406 m^2 cross-sectional area
Transmitter-loop turns	4
Transmitter-loop current	1300 A
Transmitter dipole moment	2.1×10^6 amp-m^2
Transmitter frequency	30 Hz
Receiver type	Multicoil (x, y, and z)
Receiver trailing distance	125 m behind, 50 m below
Number of recording windows	20 channels, 5 on-time, 15 off-time
Recording time (from end of pulse)	11.415 s
Sample rate	4 per s
Sample interval	17.5 m

Table A3. Specific conductance (25°C) and resistivity of surface and groundwater from the Pajarito Plateau. "Field" and "lab" refer respectively to conductivity measurements made in the field and in the laboratory. [1]For uniformity, original measurement units reported as mS/m or µS/cm are converted to mS/cm; [2]calculated from specific conductance. [3] Reported as conductivity.

Host Unit	Specific conductance (mS/cm)[1]	Resistivity (Ω-m)[2]	Location	Comments	Reference
Flowing stream water	0.1-0.9[3]	11.1-100.0	Cañon de Valle (TA-16)		LANL (2003)
Bandelier Tuff, Otowi Member	0.174	57.5	TA-16 (R-25)	Perched zone	Broxton et al. (2002a), Table 7.2-2
Cerros del Rio basalt	0.334	29.9	Mortandad Canyon (R-15)	Perched zone	Longmire et al. (2001), Table 5.2-1
Cerros del Rio basalt	0.250-0.457	21.9-40.0	Los Alamos Canyon (R-9)	Perched zone. Filtered.	Broxton et al. (2001a)
Cerros del Rio basalt	Field: 0.376-1.381 Lab: 0.429-1.381	Field: 7.24-26.6 Lab: 7.24-23.3	Sandia Canyon (R-12)	Perched zone	Broxton et al. (2001b)
"Old alluvium" between Cerros del Rio basalts and Puyé Formation	Field: 0.365 Lab: 0.434-0.443	Field: 27.4 Lab: 22.6-23.0	Sandia Canyon (R-12)	Perched zone	Broxton et al. (2001b)
Upper Puyé Formation	0.0756-0.131	76.3-132.3	Upper Los Alamos Canyon (R-7, screen #1)		Longmire and Goff (2002)
Lower Puyé Formation	0.187-0.271	36.9-53.5	Upper Los Alamos Canyon (R-7, screen #3)		Longmire and Goff (2002)
Lower Puyé Formation	0.135-0.214	46.7-74.1	Upper Los Alamos Canyon (R-7, screen #3)	Regional aquifer. Value prior to well development.	Stone et al., (2002). Table 5.0-1
Puyé Formation	0.165-0.166	60.2-60.6	TA-16 (R-25)	Perched zone	Broxton et al. (2002a), Table 7.2-2
Puyé Formation	0.133-0.151	66.2-75.2	TA-16 (R-25)	Wet/dry zone	Broxton et al. (2002a), Table 7.2-2
Puyé Formation	0.084-0.166	60.2-119.0	TA-16 (R-25)	Regional aquifer	Broxton et al. (2002a), Table 7.2-2
Puyé Formation	0.166-0.210	47.6-60.2	Mortandad Canyon (R-15)	Regional aquifer	Longmire et al. (2001), Table 5.2-1
Puyé Formation	0.192	52.1	Mortandad Canyon (R-13)	Regional aquifer. Value prior to well development.	Anonymous (2003b)
Puyé Formation	0.273-0.987	10.1-36.6	Los Alamos Canyon (R-	Perched zone	Broxton et

			9)	and regional aquifer Filtered. Parts are clay-rich	al. (2001a)
Puyé Formation	0.226	44.2	Los Alamos Canyon (R-8)	Regional aquifer. Value prior to well development. Parts are clay-rich.	Anonymous (2003c)
Puyé Formation/ Cerros del Rio basalt	0.327	30.6	MCOBT-4 4	Perched zone	Broxton et al. (2002b)
Basalt in Santa Fe Group	0.200-0.259	38.6-50.0	Los Alamos Canyon (R-9)	Regional aquifer	Longmire (2002)
Basalt in Santa Fe Group	0.160-0.272	36.8-62.5	Los Alamos Canyon (R-9i, screen #1)	Perched zone	Longmire (2002)
Basalt in Santa Fe Group	0.140-0.215	46.5-71.4	Los Alamos Canyon (R-9i, screen #2)	Perched water in vadose zone	Longmire (2002)
Basalt in Santa Fe Group	Field: 0.279 Lab: 0.277-0.284	Field: 35.8 Lab: 35.2-36.1	Sandia Canyon (R-12)	Regional aquifer	Broxton et al. (2001b)
Santa Fe Group	0.258	38.8	Pueblo Canyon (R-5)	Regional aquifer. Value prior to well development.	Anonymous (2003d)

Table A4. Electrical resistivity of hydrogeologic units of the Pajarito Plateau. [1]Calculated from conductivity. [2]Average of 29 boreholes spread across LANL, highest and lowest 2.5% of values excluded.

Unit	Conductivity (mS/m)	Resistivity (Ω/m)[1]	H_2O wt. % (gravimetric)	Location	Technique	Reference
Alluvium	~7-10.5	~95.2-142.9	5.2-7.2	Mortandad Canyon (R-15)	Array induction borehole tool	Longmire et al. (2001), Fig. 3.3-2
Bandelier Tuff, Tshirege Member	~7-23	43.5-142.9	5.2-31.1	Mortandad Canyon (R-15)	Array induction borehole tool	Longmire et al. (2001), Fig. 3.3-2
Bandelier Tuff, Tshirege Member		1454-1950	2.30-7.70	TA-36, mesa top (R-19)	Array induction borehole tool	Broxton et al. (2001c), Table 3.2-3, Append. B
Bandelier Tuff, Tshirege Member (unsaturated)		787-1386		Site-wide[2]	Array induction borehole tool	This work.
Bandelier Tuff, Tshirege Member (Tsankawi pumice bed)		830		TA-36, mesa top (R-19)	Array induction borehole tool	Broxton et al. (2001c), Table 3.2-3
Bandelier Tuff, Tshirege Member (Tsankawi pumice bed, unsaturated)		961		Site-wide[2]	Array induction borehole tool	This work.
Cerro Toledo interval		703		TA-36, mesa top (R-19)	Array induction borehole tool	Broxton et al. (2001c), Table 3.2-3
Cerro Toledo interval	11.5-33.0	30.3-87.0	10-47.4	Mortandad Canyon (R-15)	Array induction borehole tool	Longmire et al. (2001), Fig. 3.3-2
Cerro Toledo interval (unsaturated)		605		Site-wide[2]	Array induction borehole tool	This work.
Bandelier Tuff, Otowi Member		569		TA-36, mesa top (R-19)	Array induction borehole tool	Broxton et al. (2001c), Table 3.2-3
Bandelier Tuff, Otowi Member	~8.5-22.5	~44.4-117.6	14.4-22.5	Mortandad Canyon (R-15)	Array induction borehole tool	Longmire et al. (2001), Fig. 3.3-2
Bandelier Tuff, Otowi Member (vadose zone)	~4-7.5	133.3-250.0	8.29-18.72	TA-16, mesa top (R-25)	Array induction borehole tool	Broxton et al. (2002a), Fig. 5.5-2, Append. E
Bandelier Tuff, Otowi Member (perched zone)	7-11	90.9-142.9		TA-16, mesa top (R-25)	Array induction borehole tool	Broxton et al. (2002a), Fig. 5.5-2
Bandelier Tuff, Otowi Member (unsaturated)		478		Site-wide[2]	Array induction borehole tool	This work.

Bandelier Tuff, Otowi Member (Guaje pumice bed)		736		TA-36, mesa top (R-19)	Array induction borehole tool	Broxton et al. (2001c), Table 3.2-3
Bandelier Tuff, Otowi Member (Guaje pumice bed, perched zone)	>25	<40		TA-16, mesa top (R-25)	Array induction borehole tool	Broxton et al. (2002a), Fig. 5.5-2
Bandelier Tuff, Otowi Member (Guaje pumice bed, unsaturated)		807		Site-wide[2]	Array induction borehole tool	This work.
Cerros del Rio basalt, massive		156		TA-36, mesa top (R-19)	Array induction borehole tool	Broxton et al. (2001c), Table 3.2-3
Cerros del Rio basalt		100-1050		Los Alamos Canyon (R-9)	Array induction borehole tool	Broxton et al. (2001a), Figs. 5.8-1, 5.8-3, and 5.8-5
Cerros del Rio Basalt (unsat.)		343		Site-wide[2]	Array induc borehole tool	This work
Volcaniclastic sediments		268		TA-36, mesa top (R-19)	Array induction borehole tool	Broxton et al. (2001c), Table 3.2-3
Puyé Formation		74-138		TA-36, mesa top (R-19)	Array induction borehole tool	Broxton et al. (2001c), Table 3.2-3
Puyé Formation (unsaturated)		167		Site-wide[2]	Array induc. borehole tool	This work
Puyé Formation (saturated)		59		Site-wide[2]	Array induc. borehole tool	This work
Puyé Formation (perched zone)	~5-19	19.0-52.6		TA-16, mesa top (R-25)	Array induction borehole tool	Broxton et al. (2002a), Fig. 5.5-2.
Totavi Lentil (Puyé Formation) (saturated)		36		Site-wide[2]	Array induc. borehole tool	This work
Pumice-rich volcaniclastic unit (unsaturated)		150		Site-wide[2]	Array induc. borehole tool	This work
Pumice-rich volcaniclastic unit (saturated)		70		Site-wide[2]	Array induc. borehole tool	This work
Lower fanglomerate unit (saturated)		33		Array induc. borehole tool	Site-wide[2]	This work.
Santa Fe Group, undifferentiated (saturated)		16		Array induc. borehole tool	This work.	Site-wide[2]

REFERENCES

Anonymous, 2003a, Phase III RFI Report for Solid Waste Management Unit 16-021(c)-99, Los Alamos National Laboratory unpublished report, LA-UR-03-5248.

Anonymous, 2003b, Characterization well R-13 completion report, Los Alamos National Laboratory unpublished report, LA-UR-03-1373.

Anonymous, 2003c, Characterization well R-8 completion report, Los Alamos National Laboratory unpublished report, LA-UR-03-1162.

Anonymous, 2003d, Characterization well R-5 completion report, Los Alamos National Laboratory unpublished report, LA-UR-03-1600.

Archie, G.E., 1942, The electrical resistivity log as an aid in determining some reservoir characteristics, Transactions of the American Institute of Mining and Metallurgical Engineers, **146**, 54-62.

Baldridge, W. S., G. R. Keller, V. Haak, E. Wendlandt, G. R. Jiracek, and K. H. Olsen, 1995, The Rio Grande Rift, *in* K. H. Olsen, ed., Continental Rifts: Evolution, Structure , Tectonics. Elsevier, Developments in Geotectonics **25**, 233-275.

Ball, T., M. Everett, P. Longmire, D. Vaniman, W. Stone, D. Larssen, K. Greene, N. Clayton, and S. McLin, 2002, Characterization well R-22 completion report, Los Alamos National Laboratory report, LA-13893-MS.

Birdsell, K, H., B. D. Newman, D. E. Broxton, and B. A. Robinson, 2005, Conceptual models of vadose zone flow and transport beneath the Pajarito Plato, Los Alamos, New Mexico, Vadose Zone Journal, **4**, 620-636, doi:10.2136/vzj2004.0172.

Blake, W. D., F. Goff, A. I. Adams, and D. Counce, 1995, Environmental geochemistry for surface and subsurface waters in the Pajarito Plateau and outlying areas, New Mexico, Los Alamos National Laboratory report LA-12912-MS, Los Alamos, New Mexico.

Broxton, D. E., and D. T. Vaniman, 2005, Geologic framework of a groundwater system on the margin of a rift basin, Pajarito Plateau, north-central New Mexico, Vadose Zone Journal, **4**, 522-550, doi:10.2136/vzj2004.0073.

Broxton, D., R. Gilkeson, P. Longmire, J. Marin, R. Warren, D. Vaniman, A. Crowder, B. Newman, B. Lowry, D. Rogers, W. Stone, S. McLin, G. WoldeGabriel, D. Daymon, and D. Wycoff, 2001a, Characterization well R-9 completion report, Los Alamos National Laboratory report, LA-13742-MS.

Broxton, D., R. Warren, D. Vaniman, B. Newman, A. Crowder, M. Everett, R. Gilkeson, P. Longmire, J. Marin, W. Stone, S. McLin, and D. Rogers, 2001b, Characterization well R-12 completion report, Los Alamos National Laboratory report, LA-13822-MS.

Broxton, D., D. Vaniman, W. Stone, S. McLin, J. Marin, R. Koch, R. Warren, P. Longmire, D. Rogers, and N. Tapia, 2001c, Characterization well R-19 completion report, Los Alamos National Laboratory report, LA-13823-MS.

Broxton, D., R. Warren, P. Longmire, R. Gilkeson, S. Johnson, D. Rogers, W. Stone, B. Newman, M. Everett, D. Vaniman, S. McLin, J. Skalski, and D. Larssen, 2002a, Characterization well R-25 completion report, Los Alamos National Laboratory report, LA-13909-MS.

Broxton, D., D. Vaniman, P. Longmire, B. Newman, W. Stone, A. Crowder, P. Schuh, R. Lawrence, E. Tow, M. Everett, R. Warren, N. Clayton, D. Counce, E. Kluk, and

D. Bergfeld, 2002b, Characterization well MCOBt-4.4 and borehole MCOBT-8.5 completion report, Los Alamos National Laboratory report, LA-13993-MS.

Bultman, M. W., M. E. Gettings, and J. Wynn, 1999, An interpretation of the 1997 Airborne electromagnetic (AEM) survey, Fort Huachuca vicinity, Cochise County, Arizona, U.S. Geological Survey, Open-File Report 99-7-B (http://geopubs.wr.usgs.gov/open-file/of99-007-b/).

Cavazza, W., 1989, Sedimentation pattern of a rift-filling unit, Tesuque Formation (Miocene), Espanola basin, Rio Grande rift, New Mexico, Journal of Sedimentary Petrology, **59**, 287-296.

Christiansen, A. V., and N. B. Christensen, 2003, A quantitative appraisal of airborne and ground-based transient electromagnetic (TEM) measurements in Denmark: Geophysics, **68**, 523-534.

Deszcz-Pan, M., B. D. Rodriquez, J. P. Doucette, M. Godbout, J. M. Williams, D. A. Sawyer, B. D. Stone, V. J. S. Grauch, and Geoterrex-Dighem, 2001, Digital airborne time domain electromagnetic data from surveys over Cochiti Pueblo, Rio Puerco, and Rio Rancho, New Mexico, U.S.Geological Survey, Open-File Report 00-502, Ver. 1.

Gilkeson, R. H., D. E. Merewether, and C. A. Burger, 1996, The application of surface geophysical methods to characterize vadose zone hydrology in canyon settings at Los Alamos National Laboratory, Unpublished Report.

Goff, F., and S. Sayer, 1980, A geothermal investigation of spring and well waters of the Los Alamos region, New Mexico, Los Alamos National Laboratory Report, LA-8326-MS.

Ingersoll, R. V., W. Cavazza, W. S. Baldridge, and M. Shafiqullah, 1990, Cenozoic sedimentation and paleotectonics of north-central New Mexico: Implications for initiation and evolution of the Rio Grande rift, Geological Society of America Bulletin, **102**, 1280-1296.

Izett, G. A, and J. D. Obradovich, $^{40}Ar/^{39}Ar$ age constraints for the Jaramillo normal subchron and the Matuyama-Brunhes geomagnetic boundary, Journal of Geophysical Research, **99**, 2925-2934.

Keating, E. H., B. A. Robinson, and V. V. Vesselinov, 2005, Development and application of numerical models to estimate fluxes through the regional aquifer beneath the Pajarito Plateau, Vadose Zone Journal, 4, 653-671, doi:10.2136/vzj2004.0101.

Kopp, B., A. Crowder, M. Everett, D. Vaniman, D. Hickmott, W. Stone, N. Clayton, S. Pearson, and D. Larssen, 2002, Well CdV-R-15-3 Completion Report, Los Alamos National Laboratory Report LA-13906-MS.

Kopp, B., M. Everett, J. R. Lawrence, G. WoldeGabriel, D. Vaniman, J. Heikoop, W. Stone, S. McLin, N. Clayton, and D. Larssen, 2003, Well CdV-R-37-2 Completion Report, Los Alamos National Laboratory Report LA-14023-MS.

Kwicklis, E., M. Witkowski, K. Birdsell, B. Newman, and D. Walther, 2005, Development of an infiltration map for the Los Alamos area, New Mexico, Vadose Zone Journal, **4**, 672-693.

LANL, 1998, Hydrogeologic Workplan, Los Alamos National Laboratory, Los Alamos National Laboratory unpublished report LA-UR-97-329.

LANL, 2003, Phase III RFI report for SWMU 16-021 (c)-99, Los Alamos National Laboratory unpublished report, LA-UR-03-5248.

Levitt, D. G., D. L. Newell, W. J. Stone, and D. S. Wykoff, 2005, Surface water-groundwater connections at the Los Alamos Canyon weir site: Part 1. Monitoring site installation and tracer tests, Vadose Zone Journal, **4**, 708-717.

Lewis, C. J., A. Lavine, S. L. Reneau, J. N. Gardner, R. Channell, and C. W. Criswell, 2002, Geology of the western part of Los Alamos National Laboratory (TA-3 to TA-16), Rio Grande rift, New Mexico, Los Alamos National Laboratory Report LA-13960-MS.

Longmire, P., 2002, Characterization wells R-9 and R-9i geochemistry report, Los Alamos National Laboratory Report LA-13927-MS.

Longmire, P., and F. Goff, 2002, Characterization well R-7 geochemistry Report, Los Alamos National Laboratory Report LA-14004-MS.

Longmire, P., D. Broxton, W. Stone, B. Newman, R. Gilkeson, J. Marin, D. Vaniman, D. Counce, D. Rogers, R. Hull, S. McLin, and R. Warren, 2001, Characterization well R-15 completion report, Los Alamos National Laboratory Report LA-13749-MS.

McNeill, J.D., 1990, Use of electromagnetic methods for groundwater studies, *in* Ward, S.H., (ed.), Geotechnical and Environmental Geophysics, **01**, Soc. Exploration Geophysics, 191-218.

Niwas, S., P. K. Gupta, and O. A. L. Lima, 2005, Nonlinear electrical response of saturated shaly sand reservoir and its asymptotic approximations, Geophysics, in press.

Paine, J. G., 2000, Identifying and assessing ground water in the lower Rio Grande Valley, Texas, using airborne electromagnetic induction: The University of Texas at Austin, Bureau of Economic Geology, final report prepared for Texas Water Development Board, under interagency contract no. 99-483-310.

Paine, J. G., 2003, Determining salinization extent, identifying salinity sources, and estimating chloride mass using surface, borehole, and airborne electromagnetic induction methods, Water Resources Research, **39**.

Purtymun, W. D., 1984, Hydrologic characteristics of the main aquifer in the Los Alamos area: Development of ground water supplies, Los Alamos National Laboratory report LA-9957-MS.

Purtymun, W. D., 1995, Geologic and hydrologic records of observation wells, test holes, test wells, supply wells, springs, and surface water stations in the Los Alamos area, Los Alamos National Laboratory Report LA-12883-MS, Los Alamos, New Mexico.

Robinson, B. A., K. Collins, and A. M. Simmons, A. M., 2005a, Hydrogeologic synthesis report, Los Alamos National Laboratory report LA-UR-05-2814, Los Alamos, New Mexico.

Robinson, B. A., D. E. Broxton, and D. T. Vaniman, 2005b, Observations and modeling of deep perched water beneath the Pajarito Plateau, Vadose Zone J., 4, 637-652, doi: 10.2136/vzj2004.0168.

Robinson, B. A., G. Cole, J. W. Carey, M. Witkowski, C. W. Gable, Z. M. Lu, and R. Gray, 2005c, A vadose zone flow and transport model for Los Alamos Canyon, Los Alamos, New Mexico, Vadose Zone Journal, 4, 729-743.

Smith, R. S., M. D. O'Connell, and L. H. Poulsen, 2004, Using airborne electromagnetic surveys to investigate the hydrogeology of an area near Nyborg, Denmark, Near Surface Geophysics, 3, 123-130.

Stauffer, P. H., and W. J. Stone, 2005, Surface water-groundwater connection at the Los Alamos Canyon weir site: Part 2. Modeling of tracer test results, Vadose Zone Journal, 4, 718-728.

Stone, W., D. Vaniman, P. Longmire, D. Broxton, M. Everett, R. Lawrence, and D. Larssen, 2002, Characterization well R-7 report, Los Alamos National Laboratory Report LA-13932-MS.

Turbeville, B. N., D. B. Waresback, and S. Self, 1989, Lava-dome growth and explosive volcanism in the Jemez Mountains, New Mexico: Evidence from the Plio-Pleistocene Puye alluvial fan, Journal of Volcanology and Geothermal Research, 36, 267-291.

Vaniman, D., D. Broxton, and S. Chipera, 2005, Vadose zone clays and water content beneath wet and dry canyons of the Pajarito Plateau, New Mexico, Vadose Zone Journal, 4, 453-465, doi:10.2136/vzj2004.0068.

Vuataz, F. D., F. Goff, C. Fouillac, and J. Y. Calvez, 1986, Isotope geochemistry of thermal and nonthermal waters in the Valles caldera, Jemez Mountains, northern New Mexico, Journal of Geophysical Research, 91, 1835-1853.

Walters, M. C., 1996, Fracture analysis of the Bandelier Tuff, Pajarito Plateau, north-central Rio Grande rift, New Mexico: M.S. thesis, Texas Christian University.

Ward, S. H., 1990, Resistivity and induced polarization methods, *in* S. H. Ward, ed., Geotechnical and Environmental Geophysics: 01, Soc. Exploration Geophysics, 147-189.

Wohletz, K. H., 1995, Measurement and analysis of rock fractures in the Tshirege Member of the Bandelier Tuff along Los Alamos Canyon adjacent to Technical Area-21, in Broxton, D. E., and P. G. Eller, eds., Earth Science Investigations for Environmental Restoration—Los Alamos National Laboratory Technical Area 21, Los Alamos National Laboratory Report LA-12934-MS, 19-31.

Wolfgram, P., and G. Karik, 1995, Conductivity-depth transform of GEOTEM data, Exploration Geophysics, 26, 179-185.

FIGURES

Fig. 1. Location of the Los Alamos National Laboratory (LANL) on the Pajarito Plateau, adjacent to the Jemez volcanic field. The Rio Grande rift is shown by shaded pattern.

Fig. 2. Simplified chronostratigraphy of the Pajarito Plateau. Diagonally ruled pattern indicates time periods for which no rocks are represented. Modified from Broxton and Vaniman (2005).

Fig. 3. Flight lines for airborne electromagnetic survey, and boreholes for which geologic, hydrogeologic, and other data are used for this report. Flight line 112 (Fig. 6) is highlighted. Rectangular box denotes volume in which vertical sections (Fig. 7) are located. Heavy lines connecting boreholes R-12, -9, -5, and -8 and boreholes CdV-R-37-2, -R-15-3, and R-19 denote subareas 1 and 2, respectively (Figs. 8 and 14). Locations of detailed transects (Figs. 8, 14) are shown. Lozenge-shaped holes in flight-line-array are areas that, for safety or security reasons, were not overflown.

Fig. 4. Expected values of the z-component of the B-field for (A) a 20-m thick slab with lateral dimension of 2.5 x 2.5 km at depths of 200 m, 250 m, and 300m, and (B) a 20-m thick slab with lateral dimensions of 200 x 200 m at depths of 50 m, 100 m, and 150 m. Resistivity values for the slab and background are 50 Ω-m and 1000 Ω-m, respectively. Profiles are for a 30 Hz source and time windows similar to those of this survey (later times upward). Background responses are indicated by the asymptotic values at either end of the profile. The noise levels for this component are approximately 3000 fT. All amplitudes between -3000 fT and +3000 fT have been covered with the hatched box. Thus, profile lines visible are above the noise level. Cases A and B are considered proxies for, respectively, the regional water table and perched groundwater in the vadose zone. For case A, the model results indicate that a 2500 x 2500 x 20 m saturated zone (or equivalent clay layer) would be robustly imaged at depths up to 300 m. For case B, 200 x 200 x 20 m saturated zone or clay layer would yield a signature barely above background, and only in the early time windows.

Fig. 5. Conductivity-depth slices at 200 m (upper) and 300 m (lower). White regions are areas that were not overflow for safety or security reasons. Solid line is boundary of the Los Alamos National Laboratory. Dashed lines are major drainages. Location of flight line 112 (red) is shown for reference. Two northwest-southeast tie lines are indicated on both panels by colored lines. The residential/business areas of Los Alamos and White Rock, sources of particular electromagnetic noise, are indicated.

Fig. 6. Geoelectric section along flight line 112, using AirStem processing from Condor. Location is shown on Fig. 3. In this and many subsequent figures, elevations and borehole depths are presented in feet, because these are the original measurement units. A scale in meters is presented for comparison.

Fig. 7. Two vertical sections oriented approximately east-west through 3-D gridded data in part of subarea 1. Location shown on Fig. 3. 30 Ω-m contour is indicated on

both sections, with resistivity increasing upward. Sections A and B are respectively through boreholes R-9i and R-12.

Fig. 8. Correlation of AEM resistivity with clay content (left panels, saturated zones in cyan), and lithologic units (right panels) in boreholes in subarea 1 (from holes R-11, R-9/9i, R-5, and R-9). The 300 Ω-m contour from AEM is indicated for boreholes R-12 and R-9/9i, and the 30 Ω-m contour for all boreholes. Resistivity decreases downward except in upper part of R-12, where resistivity is low at surface and >300 Ω-m between depths of 18 and 46 m. No borehole resistivity is available for these holes. Cerro del Rio basalt unit is characterized by 50–75% flow interiors, 14–40% open fractures, and 4–20% clay-filled fractures. Vertical hatching in Puye Formation indicates intervals with higher abundances (up to 25 %, but typically 2–10 %) of Precambrian detritus. Location of boreholes is shown on Fig. 3. Borehole hydrogeologic data from Broxton et al. (2001a, 2001b), Longmire et al. (2002), and Anonymous (2001a, 2001b). Clay data for R-5 and R-9 from D. T. Vaniman (unpublished).

Fig. 9. Map showing region (in light blue) of clay alteration (in smectite) in the pumice rich tuffs (mafic minerals altered below the Puye Formation (see text). Most of the pumice rich unit is unaltered. Locations of selected boreholes discussed in the text are indicated. Modified from Vaniman et al. (2008).

Fig. 10. Borehole induction resistivity compared to AEM-determined resistivity (labelled AEM) (left panels), clay content (center panel), and lithologic units (right panel) at borehole R-13. Depths of geologic units, perched zones, and regional water table are in text. Pumice in the Puye Formation exposed in borehole R-13 is essentially unaltered to clay. Clay data from D. T. Vaniman (unpublished). Cerro del Rio basalt unit is characterized by 78 % flow interiors, 16 % open fractures, and 6 % clay-filled fractures. TD is total depth of borehole (in text). Regional water table is evaluated by upside down triangle. Resistivity determined by AEM is >200 Ω-m at the water table. Borehole hydrogeologic data from Anonymous (2001b).

Figs. 11. Correlation of AEM-determined resistivity (labelled AEM) with lithology (left panels), saturated zones for CDV-R-15 (and R-19 in center), and lithologic units (right panels) in boreholes in the Sierra Ciénega de Valle Grande (boreholes CDV-R-37-2, CDV-R-15-3, and R-10). Depths of geologic units, perched zones, and regional water table are in text. TD is total depth of borehole (in text). Regional water table is indicated by inverted triangle. All boreholes are monitoring wells. Locations of boreholes shown on Fig. 3. Hydrogeologic and borehole resistivity data from Koppen et al. (2002, 2001) and Broxton et al. (2001a).

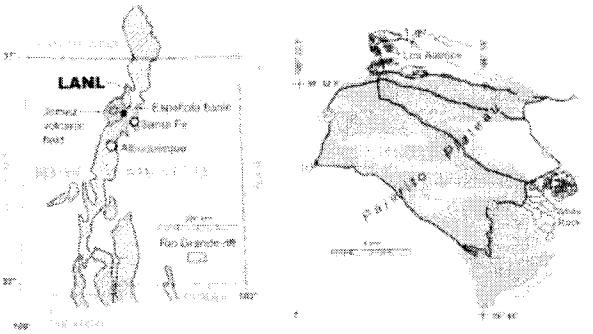

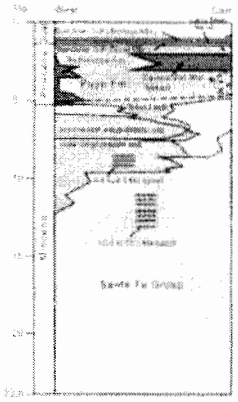

Fig. 2
Baldridge et al

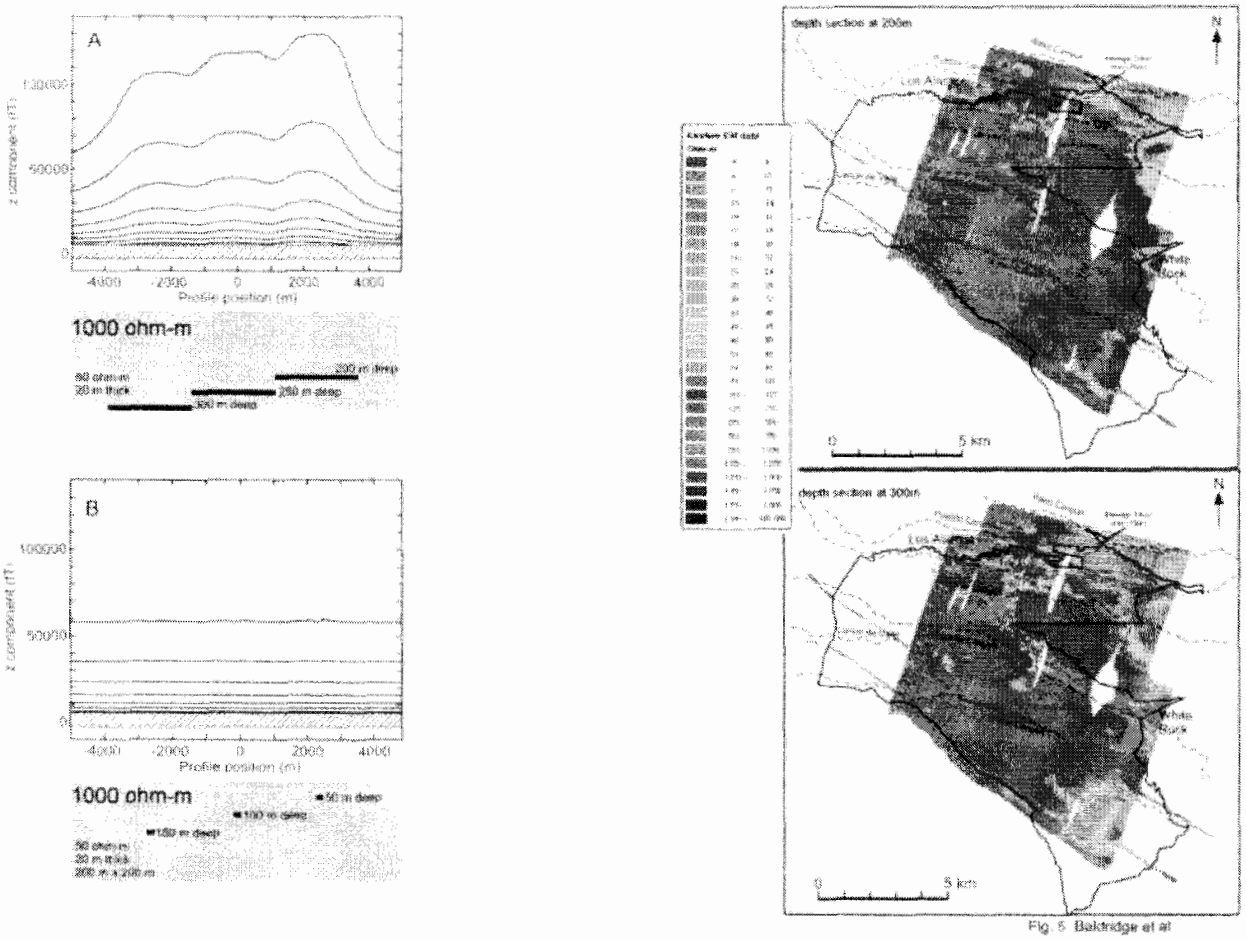

Fig. 5 Bakridge et al

Fig. 6
Baldridge et al.

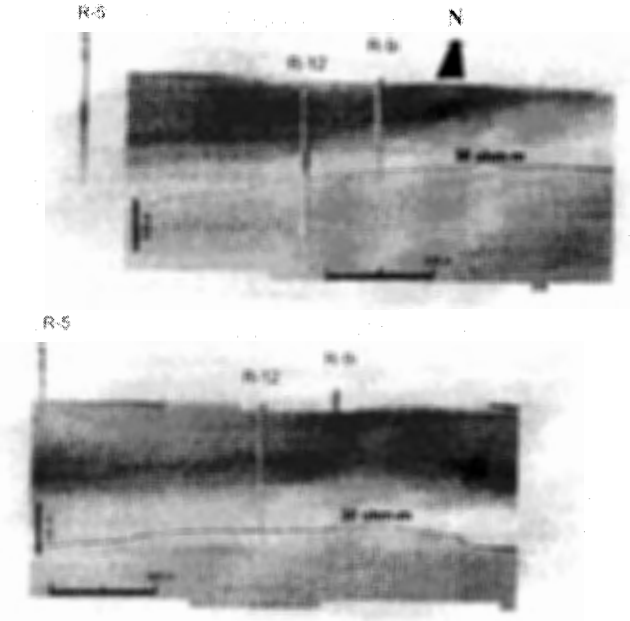

Fig. 7 Baldridge et al.

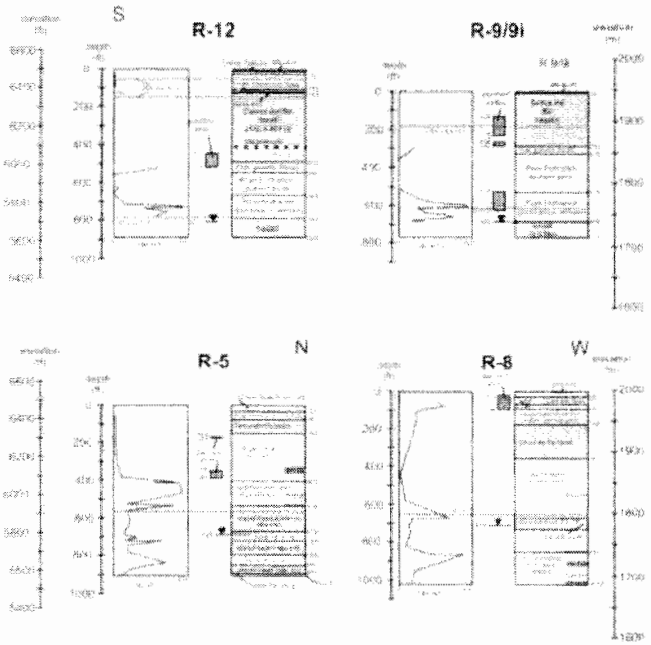

Fig. 8
Baldridge et al.

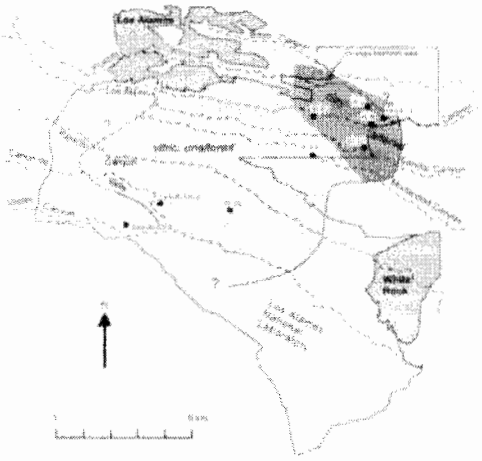

Fig. 9
BALDRIDGE ET AL

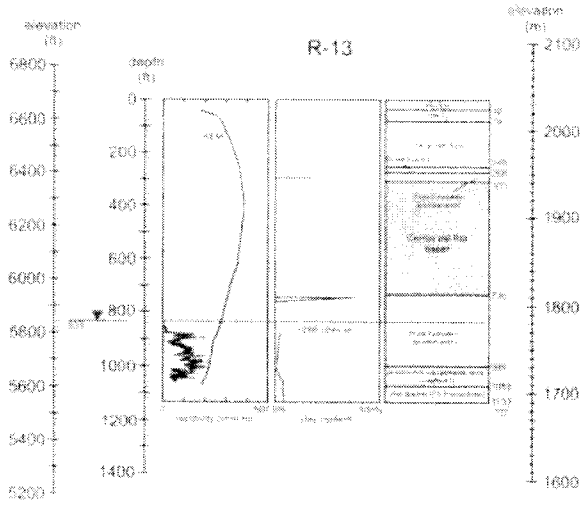

Fig. 10
BALDRIDGE ET AL.

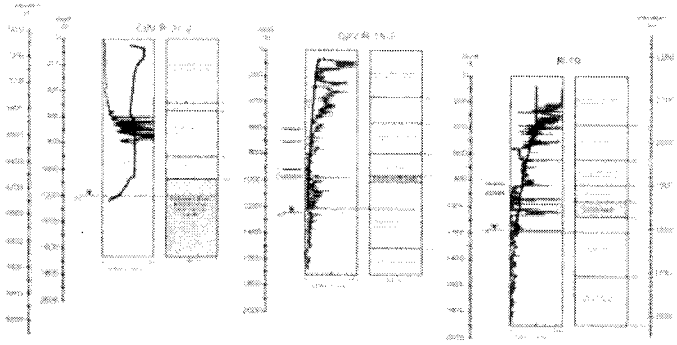

Fig. 11
Baldridge et al.